metal electrodes (Au–Ti) were patterned on appropriately selected CNT by electron-beam lithography. The diameter of the CNT was about 2 nm, as measured from atomic-force-microscopy measurement. The contact resistance was lowered by rapid thermal annealing at 800 °C for 30 s in vacuum. Half of the chosen CNTs were then covered by an SiO_2 layer of 100 nm thickness. The typical *I–V* characteristics were measured at various temperatures in vacuum. Prior to hydrogenation of the CNT, the sample was degassed for 6 h at 300 °C. Atomic hydrogen was supplied by flowing hydrogen gas through a hot tungsten filament that was located 2 cm away from the sample. This increased the sample temperature to 100 °C during hydrogenation. Hydrogenation was maintained at 10^{-5} torr for a few hours. We ensured, using atomic force microscopy, that the metal electrodes remained intact after hydrogenation. Once the hydrogenation was complete, the hydrogen supply was shut down and the chamber was evacuated again to 10^{-8} torr. The *I–V* characteristics were then measured again to see the difference.

Received: August 27, 2002
Final version: September 25, 2002

[1] a) S. Iijima, T. Ichibashi, *Nature* **1993**, *363*, 603; b) D. S. Bethune, C. H. Kiang, M. S. de Vries, G. Gorman, R. Savoy, J. Vazquez, R. Beyers., *Nature* **1993**, *363*, 605.
[2] A. Thess, R. Lee, P. Nikolaev, H. Dai, P. Petit, J. Robert, C. Xu, Y. H. Lee, S. G. Kim, A. G. Rinzler, D. T. Colbert, G. E. Scuseria, D. Tománek, J. E. Fischer, R. E. Smalley, *Science* **1996**, *273*, 483.
[3] S. J. Tans, A. R. M. Verschueren, C. Dekker, *Nature* **1998**, *393*, 49.
[4] Z. Yao, H. W. C. Postma, L. Balents, C. Dekker, *Nature* **1999**, *402*, 273.
[5] M. S. Fuhrer, J. Nygård, L. Shih, M. Forero, Y.-G. Yoon, M. S. C. Mazzoni, H. J. Choi, J. Ihm, S. G. Louie, A. Zettl, P. L. McEuen, *Science* **2000**, *288*, 494.
[6] E. T. Mickelson, I. W. Chiang, J. L. Zimmerman, P. J. Boul, J. Lozano, J. Lui, R. E. Smalley, R. H. Hauge, J. L. Margrave, *J. Phys. Chem.* **1999**, *103*, 4318.
[7] K. N. Kudin, H. F. Bettinger, G. E. Scuseria, *Phys. Rev. B: Condens. Matter* **2001**, *63*, 045 413.
[8] K. H. An, J. G. Heo, K. G. Jeon, D. J. Bae, C. Jo, C. W. Yang, C.-Y. Park, Y. H. Lee, Y. S. Lee, Y. S. Chung, *Appl. Phys. Lett.* **2002**, *80*, 4235.
[9] P. G. Collins, M. S. Arnold, P. Avouris, *Science* **2001**, *292*, 706.
[10] J.-O. Lee, C. Park, J.-J. Kim, J. Kim, J. W. Park, K.-H. Yoo, *J. Phys. D: Appl. Phys.* **2000**, *33*, 1953.
[11] B. N. Khare, M. Meyyappan, A. M. Casell, C. V. Nguyen, J. Han, *Nano Lett.* **2002**, *2*, 73.
[12] R. Martel, V. Dercke, C. Lavoie, J. Appenzeller, K. K. Chan, J. Tersoff, P. Avouris, *Phys. Rev. Lett.* **2001**, *87*, 256 805.
[13] J. Kim, J.-O. Lee, H. Oh, K. H. Yoo, J.-J. Kim, *Phys. Rev. B: Condens. Matter* **2001**, *64*, 161 404.
[14] L. C. Venema, J. W. G. Wildöer, J. W. Janssen, S. J. Tans, H. L. J. T. Tuinstra, L. P. Kouwenhoven, C. Dekker, *Science* **1999**, *283*, 52.
[15] M. Elstner, D. Porezag, G. Jungnikel, J. Elsner, M. Haugk, T. Frauenheim, S. Suhai, G. Seifert, *Phys. Rev. B: Condens. Matter* **1998**, *58*, 7260.
[16] K. A. Park, T. S. Yang, Y. H. Lee, unpublished.
[17] S. M. Lee, K. H. An, Y. H. Lee, G. Seifert, T. Frauenheim, *J. Am. Chem. Soc.* **2001**, *123*, 5059.
[18] a) C. W. Bauschlicher, *Nano Lett.* **2001**, *1*, 223. b) C. W. Bauschlicher, C. R. So, *Nano Lett.* **2002**, *2*, 337.
[19] F. Leonard, J. Tersoff, *Phys. Rev. Lett.* **2000**, *84*, 4693.
[20] J.-K. Lee, Y.-H. Cho, B.-D. Choe, K. S. Kim, H. I. Jeon, H. Lim, M. Razeghi, *Appl. Phys. Lett.* **1997**, *71*, 912.

Low-Temperature Self-Assembly of Novel Encapsulated Compound Nanowires**

By *Stephan Hofmann*,* *Caterina Ducati*, and *John Robertson**

Crystalline nanostructures, such as nanotubes and nanowires, are of great interest as they are atomically well-defined one-dimensional systems with unique features such as quantum size effects,[1] and also because they have possible uses as nanoscale devices[2–4] and tips for scanning probe microscopes.[5] An intriguing advantage of synthetic nanocrystals is their natural growth in nanometer dimensions without the need for complicated lithography processes.

Carbon nanotubes (CNTs) are one example of such nanostructures, with their structural, mechanical, and electrical properties being studied in great detail.[6] However, despite considerable progress in their assembly and integration, it is still not yet possible to control the chirality of CNTs, which determines whether they are metallic or semiconducting.[7] Furthermore, the electronic properties of CNTs are reported to change upon exposure to oxygen[8] or water vapor.[9] Therefore, alternative types of nanostructures lacking these restrictions are of great interest.

One such example are inorganic nanotubes (INTs) of transition metal dichalcogenides. These are always semiconducting and chemically inert.[10,11] In the layered MoS_2 structure, apart from tungsten as a substitutional metal, carbon was also reported to be incorporated, leading to superconducting mixed-phase nanotubes.[12] Even though stable for only a few days, nanotubes of $NiCl_2$ have also been demonstrated, and their magnetic properties evaluated.[13] Presently, a disadvantage of INTs is that they tend to require synthesis temperatures of over 900 °C, which hinders efforts on selective positioning and alignment, and this may restrict their full potential for applications.

This paper presents a versatile method to synthesize high aspect ratio nickel sulfide nanocrystals, at temperatures below 550 °C, with a high degree of positional control. We also show that the highly crystalline as-grown structures can be found encapsulated with MoS_2 layers, resulting in compound filled MoS_2 nanotubes. The result is compared to previous work involving similar pre-patterning that claimed to show crystalline arrays of single-walled CNTs of identical chirality, synthesized by annealing at high temperatures (950 °C) in a magnetic field.[14] However, it appears that the majority of structures formed were actually comparatively short Mo–C–O compounds or MoO_2.[15]

[*] Prof. J. Robertson, S. Hofmann, C. Ducati
University of Cambridge, Engineering Department
Cambridge CB2 1PZ (UK)
E-mail: jr@eng.cam.ac.uk, sh315@cam.ac.uk

[**] This work was supported by the European Union (CARBEN). We thank A. C. Ferrari and D. P. Chu for Raman and AFM measurements, respectively.

  0935-9648/02/2412-1821 $ 17.50+.50/0

ADVANCED MATERIALS

Our high aspect ratio nanocrystals were grown from patterned solid precursor materials on molybdenum substrates by annealing in a controlled atmosphere. Figure 1 shows a scanning electron microscopy (SEM) image of a 300 mesh Mo transmission electron microscopy (TEM) grid with alternating C_{60}/C_{70}–Ni layers, sublimed through a 2000 mesh Cu grid. It is clear that using commercially available TEM grids as disposable shadow masks has advantages over standard lithography, especially for patterning Mo grids. Figure 2 shows the edge of a processed Mo grid with as-grown nanocrystals originating from a heavily reacted precursor pillar, and being readily accessible for TEM analysis. The initial pillar was roughly 150 nm high, consisting of nine C_{60}/C_{70} and Ni layers with individual thicknesses varying from 40 nm to 2 nm. Annealing at 530 °C in 5 mbar nitrogen for 30 min led to the self-assembly of rod-shaped structures less than 100 nm in diameter, and more than 10 μm long.

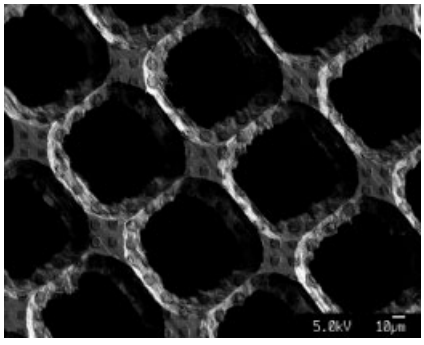

Fig. 1. SEM photograph of a 300 mesh Mo TEM grid with alternating C_{60}/C_{70}–Ni layers sublimed through a 2000 mesh Cu grid.

Fig. 2. TEM image of as-grown nanocrystals on edge of 300 mesh Mo TEM grid (scale bar 1 μm).

High-resolution (HR) TEM investigation revealed that the nanowires are highly crystalline. Although no sulfur was introduced during the patterning and synthesis process, the nanowires were identified as $Ni_xS_yC_z$ compounds by energy dispersive X-ray (EDX) and electron energy-loss spectroscopy (EELS) analysis. Sulfur is a major contaminant of commercial molybdenum grids and sheets, being adsorbed at the metal surface during wet etching. Figure 3 shows a nanowire of about 19 nm diameter, with lattice fringes of 2.92 Å parallel to the wire axis, corresponding to a $Ni_{17}S_{18}$ lattice. Carbon could occupy substitutional sites in this sulfide lattice. Figure 3 shows that there is an amorphous carbon layer on the surface of the nanowire, indicating that fullerenes can act as a carbon source, even at comparatively low temperatures. The decomposition of fullerenes might be catalytically enhanced by the presence of Ni, as reported in the literature.[16] The nanocrystals were observed to be stable, and did not suffer beam damage.

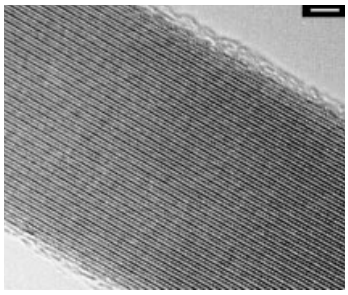

Fig. 3. HRTEM image of a portion of a nanowire of 19 nm in diameter. Lattice fringes parallel to the wire axis of 2.92 Å can be seen, corresponding to that of a $Ni_{17}S_{18}$ lattice. Carbon can occupy substitutional sites in the sulfide lattice, and is present at the surface of the nanocrystal (scale bar 2 nm).

Analyzing nanostructures on processed-patterned, sulfur-contaminated Mo grids by HRTEM, we found not only high aspect ratio sulfide nanocrystals, but also layers of MoS_2 surrounding these structures. Figure 4 shows such a heterostructure synthesized at 550 °C in 10 mbar nitrogen in 1 h. The nanowire has a diameter of ~23 nm. Figure 4a shows a set of 14 walls parallel to the wire axis, and a core that is filled with a highly crystalline material. The outer walls with the characteristic spacing of 6.2 Å are identified as MoS_2. The lattice fringes of the core of the nanowire correspond to the 3.10, 2.85, and 2.72 Å spacings of $Ni_{17}S_{18}$. EEL spectra acquired at the periphery, as well as at the central part of the wire, confirm its composite nature (Fig. 4b). Reported growth models of metal dichalcogenide nanostructures suggest the layered structures form by sulfur replacing oxygen on the oxide surface,[17] however no oxygen was detected in the nanostructures. Carbon is found both in the outer walls and in the core of the wire, and very little amorphous carbon was observed surrounding the nanocrystal. It is reasonable to suppose that carbon atoms form a misfit compound within the MoS_2 layered structure,[12] and that it occupies substitutional sites in the $Ni_{17}S_{18}$ lattice. Raman spectra of the filled MoS_2 structures closely resemble the previously published signals of platelet MoS_2 samples.[18]

The growth process was further studied by taking various different stacking orders within the pillars of the precursor materials, starting with substrates carrying solely one precursor. Under identical processing conditions, neither pure patterned Ni, nor just C_{60}/C_{70} sublimed through a 2000 mesh Cu grid, led to any high aspect ratio crystals. On the other hand, one Ni layer sandwiched between two C_{60}/C_{70} layers yields long nanowires, almost as long as from the multi-layered pre-

  0935-9648/02/2412-1822 $ 17.50+.50/0 *Adv. Mater.* **2002**, *14*, No. 24, December 17

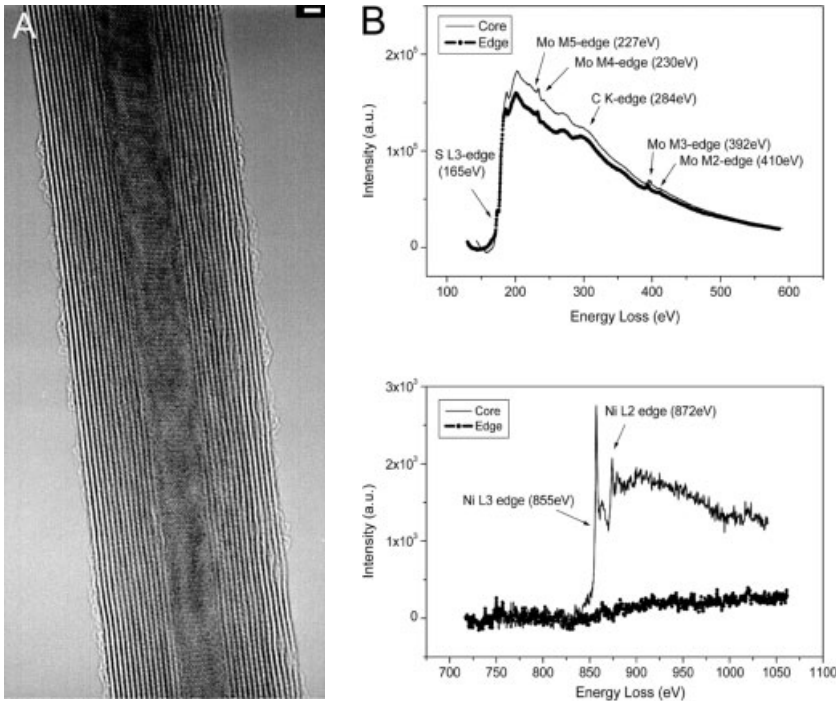

Fig. 4. a) HRTEM image of a compound filled MoS_2 nanotube 23 nm in diameter. A set of 14 outer walls parallel to the wire axis with the characteristic spacing of 6.2 Å can be seen. The lattice fringes of the nanotube core correspond to the 3.10, 2.85, and 2.75 Å spacings of $Ni_{17}S_{18}$. Carbon is found both in the outer walls and in the core of the wire (scale bar 2 nm). b) EELS spectra of the edge and core of the filled MoS_2 nanotube, showing the region of S, C, and Mo ionization edges (top), and the Ni ionization edges (bottom). The absence of the Ni peak from the spectrum acquired at the outer walls confirms the heterogeneous structure of the nanowire.

cursor structure described above. It is interesting to note that processing pure fullerite pillars leaves hardly any material on the pattern, suggesting that Ni acts as a sublimation barrier. To study the effect of the annealing atmosphere, the vacuum chamber was kept at base pressure during processing, rather than being refilled with nitrogen. Despite identical pre-patterning, a vacuum treatment was found to be less efficient for nanowire formation.

Some multi-layered C_{60}/C_{70}–Ni patterns were heated to 950 °C in vacuum for up to an hour, as in the work by Schlittler et al.[14] We found that nanorods began to emerge perpendicularly from the surface, even without an external magnetic field. They are highly crystalline, up to 1 μm long, and typically 100 nm in diameter, as previously found.[14,15] However, not only are these crystals significantly shorter than the nanowires grown at lower temperatures, but we also found them to grow preferentially in between the precursor pillars. This explains why there is no Ni incorporation, and the reported structures are found to be Mo–C–O compounds or MoO_2,[15] which tends to form short rod-like structures. Similar to other groups, we can not verify the synthesis of single-walled CNT crystals with this method.[14]

Any synthesis method for future applications using integration of nanostructures requires the ability to select the growth position and orientation. Figure 5 shows self-assembled nanostructures originating from multi-layered C_{60}/C_{70}–Ni patterns on a Mo sheet processed at 510 °C in 5 mbar nitrogen for 30 min. By covering the top of the precursor pillar with a thick Ni layer (or other suitable metal), the nanowires now emerge from the side of the pillar, showing the potential of selective lateral growth. Within a general growth model, we are presently investigating the use of different substrate materials, other transition metals such as Co and Fe, and various ways of supplying sulfur. It is particularly interesting to integrate with silicon technology, by using silicon wafers as substrate material, and supplying the Mo as additional layer in the precursor pillars.

In conclusion, we have shown a simple, low temperature synthesis route for nickel sulfide nanowires and compound-filled MoS_2 nanotubes. The effects of precursor preparation and annealing conditions were discussed. The feasibility of selective positioning and alignment may allow these nanowires and filled inorganic tubules to open new fields of applications, such as nano-templates and novel precision probes for scanning microscopy. As ferromagnetic metals are incorporated or encapsulated, novel magnetic probes and data storage devices are also possible. Furthermore, probing their electrical transport properties, such as magnetoresistance and superconductivity, may bring new fundamental insights.

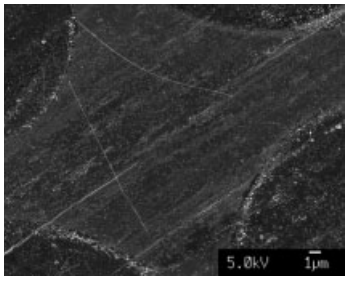

Fig. 5. SEM photograph of self-assembled nanostructures originating from multilayered C_{60}/C_{70}–Ni patterns on a Mo sheet processed at 510 °C in 5 mbar nitrogen for 30 min. The modified precursor pillars only allow lateral growth originating from the pillar edge.

Experimental

Pillars of alternating C_{60}/C_{70} and Ni layers were formed by evaporating C_{60}/C_{70} powder (fullerite, Sigma-Aldrich) and Ni metal (99.99 %) from tungsten boats mounted on a four turret source in a standard evaporator. The fullerite powder was degassed for several minutes before sublimation. The system was allowed to reach its base pressure of 10^{-6} mbar again after the deposition of each C_{60}/C_{70} or Ni layer. The films were condensed onto either 300 mesh Mo TEM grids (Agar Scientific) or plain Mo sheets. The deposited materials were patterned by using various Cu TEM grids as shadow masks, the highest mesh (2000) leading to a 10 μm × 10 μm feature size with a 10 μm pitch. The patterning dimensions and thickness of individual layers were verified by atomic force microscopy (AFM, Digital Instruments Nanoscope III). The as-prepared sam-

  0935-9648/02/2412-1823 $ 17.50+.50/0

ADVANCED MATERIALS

ples were transferred to a vacuum system fitted with a ceramic heating element (Elstein-Werk). After evacuation to below 10^{-6} mbar, the chamber was refilled with nitrogen (5.0 grade), and the samples were typically processed at 5–10 mbar and 510–550 °C for up to 1 h. Alternatively, some pre-patterned samples were annealed at 950 °C in a vacuum furnace (base pressure 10^{-6} mbar) for times varying from a few minutes to an hour. The structure and composition of the nanocrystals were analyzed by a combination of scanning electron microscopy (SEM, Jeol 6340 FEGSEM), high-resolution transmission electron microscopy (HRTEM, Jeol JEM 4000EX, 400 kV), energy dispersive X-ray spectroscopy (EDX), electron energy loss spectroscopy (EELS, VG HB501 STEM, 100 kV), and Raman spectroscopy (Renishaw RM series).

Received: July 8, 2002
Final version: September 27, 2002

[1] M. Bockrath, D. H. Cobden, J. Lu, A. G. Rinzler, R. E. Smalley, L. Balents, P. L. McEuen, *Nature* **1999**, *397*, 598.
[2] P. G. Collins, A. Zettl, H. Bando, A. Thess, R. E. Smalley, *Science* **1997**, *278*, 100.
[3] G. Y. Tseng, J. C. Ellenbogen, *Science* **2001**, *294*, 1293.
[4] S. J. Wind, J. Appenzeller, R. Martel, V. Derycke, P. Avouris, *Appl. Phys. Lett*. **2002**, *80*, 3817.
[5] A. Rothschild, S. R. Cohen, R. Tenne, *Appl. Phys. Lett*. **1999**, *75*, 4025.
[6] M. S. Dresselhaus, G. Dresselhaus, P. Avouris, *Carbon Nanotubes*, Springer, Berlin **2000**.
[7] R. Saito, M. Fujita, G. Dresselhaus, M. S. Dresselhaus, *Phys. Rev. B* **1992**, *46*, 1804.
[8] P. G. Collins, K. Bradley, M. Ishigami, A. Zettl, *Science* **2001**, *287*, 1801.
[9] A. Zahab, L. Spina, P. Poncharal, C. Marliere, *Phys. Rev. B* **2000**, *62*, 10 000.
[10] Y. Feldmann, E. Wassermann, D. J. Srolovitz, R. Tenne, *Science* **1995**, *267*, 222.
[11] G. L. Frey, S. Elani, M. Homyonfer, Y. Feldmann, R. Tenne, *Phys. Rev. B* **1998**, *57*, 6666.
[12] W. K. Hsu, Y. Q. Zhu, C. B. Boothroyd, I. Kinloch, S. Trasobares, H. Terrones, N. Grobert, M. Terrones, R. Escudero, G. Z. Chen, C. Colliex, A. H. Windle, D. J. Fray, H. W. Kroto, D. R. M. Walton, *Chem. Mater*. **2000**, *12*, 3541.
[13] Y. Rosenfeld Hacohen, E. Grunbaum, R. Tenne, J. Sloan, J. L. Hutchison, *Nature* **1998**, *395*, 336.
[14] R. R. Schlittler, J. W. Seo, J. K. Gimzewski, C. Durkan, M. S. M. Saifullah, M. E. Welland, *Science* **2001**, *292*, 1136.
[15] C. Durkan, A. Ilie, M. S. Saifullah, M. E. Welland, *Appl. Phy. Lett*. **2002**, *80*, 4244.
[16] N. Grobert, M. Terrones, A. J. Osborne, H. Terrones, W. K. Hsu, S. Trasobares, Y. Q. Zhu, J. P. Hare, H. W. Kroto, D. R. M. Walton, *Appl. Phys. A* **1998**, *67*, 595.
[17] Y. Feldmann, G. L. Frey, M. Homyonfer, V. Lyakhovitskaya, L. Margulis, H. Cohen, G. Hodes, J. L. Hutchison, R. Tenne, *J. Am. Chem. Soc*. **1996**, *118*, 5362.
[18] G. L. Frey, R. Tenne, M. J. Matthews, M. S. Dresselhaus, G. Dresselhaus, *Phys. Rev. B* **1999**, *60*, 2883.

Macroporous Silica From Solid-Stabilized Emulsion Templates**

By *Bernard P. Binks**

The use of surfactant-stabilized foams or emulsions as templates for the preparation of porous materials has been described by several authors.[1–4] These find wide application as lightweight structural materials, sorption media, filters, and catalysts. Wu et al.[1] synthesized cellular silica and mullite (alumina–silica ceramic) by foaming sol–gel dispersions, using freon and surfactant mixtures, with subsequent removal of the gas by drying and sintering. The average cell sizes ranged from 30 to 1000 μm. Monodisperse macroporous materials of titania, zirconia, and silica, with pore sizes ranging from 50 nm to several micrometers, were prepared by Imhof and Pine[2] by first mixing a monodisperse emulsion of oil-in-formamide with the metal oxide sol in formamide, followed by gelling the continuous sol phase. Subsequent drying and heat treatment yielded solid materials with spherical pores left behind by the emulsion drops. This procedure was modified for oil-in-water (o/w) emulsions by Yi and Yang,[3] although a non-uniform distribution of pores in silica resulted. High internal phase emulsions of supercritical carbon dioxide-in-water have recently been employed as templates for the production of porous polymers, with pore sizes around a few micrometers.[4] Unlike other solvents that may be difficult to remove completely, supercritical CO_2 is non-toxic, non-flammable, and reverts to the gaseous state upon de-pressurization. Unfortunately, conventional surfactants do not adsorb at its interface with water, and exotic fluoro-containing surfactants need to be synthesized specially.

We describe here a simple and effective way of preparing porous silica arising from emulsions stabilized by silica particles alone, i.e., in the absence of surfactant. Evaporation in air of such emulsions gives rise to solids with varying degrees of porosity and inherent wettability. It is believed that the chemical nature of the fumed silica particles is the key to this process, which is feasible for a wide range of emulsion composition. The surfaces of the silica particles employed contain silanol (SiOH) groups, which impart hydrophilic character. By reacting them with a silane reagent, a proportion of these groups can be converted to dimethyl end groups rendering the particles more hydrophobic. Emulsions stabilized by solid particles were reported by Ramsden[5] and Pickering[6] nearly a hundred years ago, and although this area of research lay dormant for many years, there has been a revival of interest in it recently. This includes, in particular, the work of Tambe and Sharma,[7] Zhai and Efrima,[8] and Midmore,[9] although in these studies particles are employed in addition to other surface-active agents. The present work extends the recently reported studies on the preparation, type and stability of oil+water emulsions using nanoparticle fumed silica as the sole stabilizer,[10] and the detailed study of the mechanism of evaporation from surfactant-stabilized o/w emulsions.[11] In particular for the former, the influence of the particle wettability at the oil–water interface, varied by using particles of different controlled hydrophobicity, was investigated.[12] Solid particles can function in similar ways to surfactant molecules, with the relevant parameter in the case of spherical particles being the contact angle, θ, which the particle makes with the interface. For hydrophilic particles, e.g., metal oxides, θ measured into the aqueous phase is normally $< 90°$, and preferred emulsions (equal volumes of oil and water) are o/w. For

[*] Dr. B. P. Binks
Surfactant & Colloid Group, Department of Chemistry
University of Hull, Hull HU6 7RX (UK)
E-mail: b.p.binks@hull.ac.uk

[**] The author thanks Dr. H. Barthel of Wacker-Chemie (Munich) for supplying the silica powders, A. Sinclair (University of Hull) for the SEM measurements on solids and M. Kirkland (Unilever, Colworth) for the freeze fracture SEM measurements on emulsions.

